Isotropic theoretical angular correlation of annihilation radiation spectra for positrons trapped at an Al surface?

1989 J. Phys.: Condens. Matter 1 9243

(http://iopscience.iop.org/0953-8984/1/46/016)

J. Phys.: Condens. Matter **1** (1989) 9243–9259. Printed in the UK

Isotropic theoretical angular correlation of annihilation radiation spectra for positrons trapped at an Al surface?

A Rubaszek and J Lach

Institute of Low Temperature and Structure Research, Polish Academy of Sciences, 50-950 Wrocław 2, PO Box 937, Poland

Received 6 December 1988, in final form 28 April 1989

Abstract. The electronic properties of an Al surface are computed within the jellium model. The positron annihilation characteristics are calculated for a correlated electron–positron system using the Kahana-type momentum-dependent enhancement factors in a local way. For the first time, the change of the anisotropy direction in the shape of theoretical angular correlation of annihilation radiation spectra for positrons trapped at an Al surface is obtained. The resulting momentum distribution is almost isotropic, in agreement with experimental data.

1. Introduction

A beam of mono-energetic positrons, in the energy range from below 1 eV up to a few tenths of a kiloelectronvolt, is a new tool to probe the electronic properties of metal surfaces. Interest in experiments with low-energy positrons (for reviews see, e.g. Mills 1983, Dupasquier and Zecca 1985) has increased in the last few years, since the production of the first usable beam of slow positrons and the measurement of their interaction with a metal surface by Canter *et al* (1974). Particularly, the well known angular correlation of annihilation radiation (ACAR) technique (for a review see West 1974) appears promising for momentum spectroscopy of electron surface states.

Resent measurement of 2γ ACAR from a 99.9999% clean Al(100) surface, performed by Lynn *et al* (1985) using a beam of 200 eV positrons, showed a surprising result: the momentum distribution of annihilating pairs identified with the positron surface state had nearly isotropic shape. The full width at half-maximum (FWHM) of ACAR spectra was equal to 7.1 ∓ 0.5 mrad for both directions—parallel and perpendicular to the surface. On the other hand, the majority of these spectra calculated theoretically until now for the Al surface showed an anisotropy, with momentum perpendicular to the surface ($p_\perp$) broader than the parallel ($p_\parallel$) component. The only exceptions are the results of Brown *et al* (1988a, b) and Lou Yongming (1988), both obtained within independent-particles model (IPM) (the possibilities of this isotropy are discussed by Rubaszek (1989)).

The theoretical calculations of slow positron interaction with a metal surface are based on two alternative models: (i) the surface positron is assumed to be a positronium (Ps) weakly bound to the surface by van der Waals forces (Platzman and Tzoar 1986); or (ii) the positron is tightly bound to the surface in the image-induced correlation

0953-8984/89/469243 + 17 $02.50

potential well (Hodges and Stott 1973, Nieminen and Manninen 1974, Rozenfeld *et al* 1983, Brown *et al* 1987, 1988a, b, Lou Yongming 1988).

The approach of Platzman and Tzoar (1986) appeared to be very advantageous because it led to results for positron lifetime τ and binding energy E_B in excellent agreement with experimental data (Lynn *et al* 1984, Mills and Pfeiffer 1979, respectively). In particular, the theoretical value $\tau = 580$ ps (i.e. about 15% longer than the lifetime of a free positronium atom) was obtained by these authors, for the first time based on more physical grounds than any *ad hoc* procedure assuming an unphysical cut-off in local annihilation rate. The deficiency of the Platzman–Tzoar formalism, however, consists of the fact that reactive atoms do not physisorb on metals and that the model neglects the pick-off processes, important for Ps annihilation. It should also be pointed out that the ACAR spectra (which are the centre of interest of the present work) have not been calculated explicitly by Platzman and Tzoar (1986) but only predicted. In the direction parallel to the surface, the shape of the angular correlation was simply related to the Fourier transform of the wavefunction of the system, i.e. approximately Lorentzian squared with FWHM equal to $2\langle p^2\rangle_{\perp}^{1/2} \simeq 4.8$ mrad. In the direction perpendicular to the surface, the momentum distribution was not determined by these authors and the FWHM was only predicted to be equal to about 4.8 mrad.

The effective calculations of ACAR from an Al surface performed within the model of a positron trapped in the potential well are based either on the independent-particles model (IPM) (Rozenfeld *et al* 1983, Lou Yongming 1988) or on the mixed-density approximation (MDA) (Nieminen and Manninen 1974, Brown *et al* 1987, 1988a, b). It should be mentioned here that the MDA (introduced by Arponen *et al* 1973), which turned out to be very efficient for investigating positron annihilation at lattice defects, seems to be rather controversial in the case of positron interaction with a metal surface because of the infinite size of vacuum, treated as a large void. This fact will be discussed in detail in § 2.3 (see also Rubaszek 1989). Moreover, in contradiction to the positronium model, almost all the ACAR spectra obtained within this second formalism for the correlated system were anisotropic for the Al surface, with the distribution of momentum perpendicular to the surface, $N(p_{\perp})$, broader than the parallel one, $N(p_{\parallel})$ (this anisotropy varies from 10% to 50%). It is difficult to reconcile this result with the slow-positron experiment of Lynn *et al* (1985). The only exceptions are the isotropic IPM spectra obtained by Lou Yongming (1988) for a very simple electron model potential and those by Brown *et al* (1988a, b), contradicting their previous strong anisotropic IPM result (Brown *et al* 1987). We would like to mention here that the possibilities of full isotropy of IPM surface ACAR spectra are discussed by Rubaszek (1989) using the autocorrelation function method. This isotropy appeared to be strongly dependent on the translational properties of the electron and positron wavefunctions perpendicular to the surface. It should also be pointed out that the IPM, neglecting electron–positron correlations, cannot be treated as satisfactory for the surface problem. Near the surface the electron density rapidly decreases and the effect of these correlations is pronounced. Therefore, it should be included into the formalism while calculating surface ACAR spectra.

Finally it should be noted here that there is a discrepancy (as concerns the anisotropy of ACAR spectra from an Al surface) not only between various theories and between theory and experiment, but also between various experiments. Ewertowski and Świątkowski (1987) performed an experiment with a multilayer Al/Al_xO_y foil using fast positrons and obtained an anisotropic shape of ACAR spectra. However, in this case there is uncertainty concerning the fraction of positrons diffusing to the surface and the

fraction annihilating in the bulk material. Moreover, positronium should not be formed in the interface region.

The shape of theoretical ACAR spectra from a metal surface is still an open problem and there is a real need to determine these spectra within the reliable fully correlated electron–positron model. In the present work some attempt in this direction is made. We have abandoned the approach of Platzman and Tzoar (1986) because the ACAR coming from this formalism does not reflect the electron momentum distribution (Walker and Nieminen 1986). The ACAR spectra were calculated by us within the model of a positron bound to the surface in its image–correlation well, but in a new way, beyond MDA. The differences between the present approach and the MDA are that the density of electrons on the positron is enhanced not only locally (as in MDA) but also separately for particular electronic states as well as that the exact form of the electron wavefunctions is used instead of the plane waves assumed in MDA (as is discussed by Rubaszek (1989)).

Using the present formalism instead of MDA is substantiated by the fact that ACAR spectra yield information about the separate electronic states, while calculations within MDA are based on total density of electrons and (incorrect at the surface region) the assumption that electron wavefunctions are in the form of plane waves. Applying the local enhancement factors (Daniuk *et al* 1985, 1987) of Kahana type (Rubaszek and Stachowiak 1988) leads to reversal of anisotropy (with respect to IPM) with $N(p_\parallel)$ only slightly broader than $N(p_\perp)$ and allows one to predict the isotropic shape of ACAR spectra, in agreement with the experimental data of Lynn *et al* (1985).

2. Formalism

Our calculations are performed within the jellium model, where the ions are thought of as forming a constant positive background charge within the metal (and to be confined to the negative half-space):

$$\rho_{\text{ion}}(z) = \begin{cases} \rho_0 & z \leqslant 0 \\ 0 & z > 0 \end{cases}$$

where $\rho_0 = 3/(4\pi r_s^3)$ is the electron density in the bulk material and r_s is the Wigner–Seitz radius (for Al, $r_s = 2.07$). The z axis is perpendicular to the surface and the vacuum is located in the positive half-space, $z > 0$. Atomic units are used throughout: $h = m = e = 1$.

2.1. Electrons at the surface

In the absence of a positron the (unnormalised) electron wavefunctions $\psi_k^0(\boldsymbol{r})$ are assumed in the form

$$\psi_k^0(\boldsymbol{r}) = \exp[\mathrm{i}(k_x x + k_y y)]\psi_{k_z}(z) \tag{1}$$

where $\boldsymbol{r} = [x, y, z]$. Functions $\psi_{k_z}(z)$ obey the set of Schrödinger equations:

$$\left(-\frac{\mathrm{d}^2}{\mathrm{d}z^2} + 2V_{\text{eff}}(z)\right)\psi_{k_z}(z) = (k_z^2 - k_{\text{F}}^2)\psi_{k_z}(z) \tag{2}$$

with boundary conditions

$$\psi_{k_z}(\infty) = 0 \qquad \text{and} \qquad \psi_{k_z}(-\infty) = \sin[k_z z + \gamma(k)]$$

where the phase shifts $\gamma(k)$ are continuous and $\gamma(0) = 0$. In equation (2) k_{F} denotes the

Fermi momentum of the bulk material, corresponding to r_s. According to the condition of the neutrality of the metal, the $\gamma(k)$ satisfy the Sugiyama–Langreth (Langreth 1972) phase-shift rule:

$$(2/k_F^2)\int_0^{k_F} k\gamma(k)\,dk = \pi/4.$$

In equation (2) V_{eff} is an effective potential acting on electrons, and consists of electrostatic (V_C) and exchange–correlation (V_{xc}) parts:

$$V_{eff}(z) = V_C(z) + V_{xc}(z). \tag{3}$$

The Coulomb potential V_C satisfies the Poisson equation with respect to the electron density, $\rho(z)$:

$$\frac{d^2}{dz^2}V_C(z) = -4\pi[\rho(z) - \rho_{ion}(z)] \tag{4}$$

where

$$\rho(z) = (1/\pi^2)\int_0^{k_F}(k_F^2 - k_z^2)[\psi_{k_z}(z)]^2\,dk_z. \tag{5}$$

In this work equations (2)–(5) were solved self-consistently within the iterative scheme proposed by Manninen *et al* (1975) and adapted to the finite space by Monnier and Perdew (1978). In the $(n+1)$th iterative step the potential V_C^{n+1} was determined, based on the values of electron density $\rho^n(z)$ obtained in the nth step, according to the formula

$$\begin{aligned} V_C^{n+1}(z) = [1/(2K)]\int_\alpha^\beta dz_1\{4\pi[\rho^n(z_1) - \rho_{ion}(z_1)] + KV_C^n(z_1)\}\exp(-K|z - z_1|) \\ + \tfrac{1}{2}\{V_C^n(\alpha) - (1/K)[V_C^n]'(\alpha)\}\exp(-K|z - \alpha|) \\ + \tfrac{1}{2}\{V_C^n(\beta) - (1/K)[V_C^n]'(\beta)\}\exp(-K|\beta - z|) \end{aligned} \tag{6}$$

where $[V_C^n]'(z) = (d/dz)V_C^n(z)$ and K is a constant securing the convergence of the procedure. In our calculations we chose $\alpha = -7\pi/k_F$, $\beta = 3\pi/k_F$ (outside of this region $\delta\rho(z) = \rho(z) - \rho_{ion}(z)$ is negligible) and $K = k_F$. The potential V_C was scaled to the bulk chemical potential inside the metal (i.e. $V_C(z) = \frac{1}{2}k_F^2 + V_{xc}(\rho_0) = \mu$ for $z < \alpha$).

In our calculations the electron–electron correlations and exchange are treated in a local way, i.e. neglecting all the terms proportional to the gradients of the density, and they are given by

$$V_{xc}[\rho(z)] = \frac{d}{d\rho}[\rho\varepsilon_{xc}(\rho)]_{\rho=\rho(z)}$$

where $\varepsilon_{xc}(\rho)$ is the exchange and correlation energy per particle in the electron gas of density $\rho(z)$. In this work ε_{xc} was in Wigner's form (Pines 1963), where the density of homogeneous electron gas was replaced by its local value

$$\varepsilon_{xc}[\rho(z)] = -\frac{0.458}{r_s(z)} - \frac{0.44}{r_s(z) + 7.8}.$$

Here $r_s(z) = [\frac{4}{3}\pi\rho(z)]^{-1/3}$. It was verified that using the other approximations for ε_{xc}

(e.g. Gunnarson *et al* 1979, Ceperley and Alder 1980) affects the results only very slightly (within a few per cent).

2.2. *Positron wavefunction*

At zero temperature the positron has zero momentum parallel to the surface and its ground-state wavefunction is in the form

$$\psi_+(\boldsymbol{r}) = \psi_+(z). \tag{7}$$

The (normalised) wavefunction $\psi_+(z)$ is the solution of the one-dimensional Schrödinger equation

$$\left(-\frac{\mathrm{d}^2}{\mathrm{d}z^2} + 2V_+(z)\right)\psi_+(z) = 2E_+\psi_+(z)$$

with boundary conditions $\psi_+(\mp\infty) = 0$ and $\psi'_+(\mp\infty) = 0$. Here $E_+ = E_B - \Phi_+$, where E_B is the binding energy relative to vacuum, Φ_+ is the positron work function and $V_+(z)$ is a positron potential. In this work V_+ was determined, based on the values of electrostatic potential $V_C(z)$, in the way proposed by Brown *et al* (1987). First, the positron potential V_p was defined as

$$V_p(z) = -V_C(z) + E_{corr}(r_s(z))$$

where E_{corr} is the electron–positron correlation energy, taken in this work in the form (Bhattacharyya and Singwi 1972)

$$E_{corr}(r_s) = 0.25 + 6.1\exp[-0.965(r_s - 1)].$$

It should be pointed out that V_p is not determined self-consistently. Therefore, in order to ensure that the electron–positron potential V_+ has the correct vacuum limit ($V_+(\infty) = -0.25$ au $= -6.8$ eV) and that in the bulk material it is equal to the negative positron work function $|\Phi_+|$ ($V_+(-\infty) = -\Phi_+ = 0.19$ eV (Mills 1983 and references therein)), V_p is scaled to give

$$V_+(z) = A[V_p(z) + 0.25] - 0.25$$

where

$$A = (0.25 - \Phi_+)/[0.25 + V_p(-\infty)].$$

At large distances from the surface V_+ is given by the shifted image potential (Nieminen and Manninen 1974):

$$V_+(z) = -1/[4(z - z_I)]$$

where the shift in the image plane, z_I, for aluminium is equal to 1.6 au. This image potential is truncated at z_0, where it intersects with the correlation potential.

2.3. *ACAR spectra*

The momentum distribution of annihilating pairs is given by the well known formula

$$N(\boldsymbol{p}) = \sum_{k_{\mathrm{occ}}} \left| \int \exp(-\mathrm{i}\boldsymbol{p}\cdot\boldsymbol{r})\psi_k^{\mathrm{ep}}(\boldsymbol{r},\boldsymbol{r})\,\mathrm{d}\boldsymbol{r} \right|^2 \tag{8}$$

where $\boldsymbol{p} = [p_x, p_y, p_z]$ and $\psi_k^{\mathrm{ep}}(\boldsymbol{x}_e, \boldsymbol{x}_p)$ is the pair wavefunction of the thermalised positron at $\boldsymbol{x}_p$ and the electron in the initial state $\boldsymbol{k}$ located at $\boldsymbol{x}_e$. The summation in equation (8) is over all occupied electronic states $\boldsymbol{k}$.

In the IPM, $\psi_k^{\mathrm{ep}}(\boldsymbol{r},\boldsymbol{r}) = \psi_+(\boldsymbol{r})\psi_k^0(\boldsymbol{r})$ and, taking into account the forms (1) and (7) of ψ_k^0 and ψ_+, formula (8) simplifies to

$$N^{\mathrm{IPM}}(\boldsymbol{p}) = \int_0^{\gamma} \mathrm{d}k_z \left| \int_{-\infty}^{\infty} \exp(-\mathrm{i}p_z z)\,\psi_+(z)\,\psi_{k_z}(z)\,\mathrm{d}z \right|^2. \tag{9}$$

where $\gamma = (k_{\mathrm{F}}^2 - p_x^2 - p_y^2)^{1/2}$.

However, it is well known that electron density on the positron is strongly enhanced from its initial value. Therefore, IPM is not satisfactory and electron–positron correlations cannot be neglected in equation (8). MDA includes these correlations in the average and for the jellium surface leads to the momentum distribution in the form (Brown *et al* 1987):

$$N(\boldsymbol{p}) = \int_{-\infty}^{\infty} \mathrm{d}R_z \int_0^{\infty} \mathrm{d}z \cos(p_z z)\psi_+(z_1)\psi_+(z_2)\Gamma[\rho(R_z)]\sin(\kappa z)/[z k_{\mathrm{F}}^3(R_z)] \tag{10}$$

where $\kappa = [k_{\mathrm{F}}^2(R_z) - p_x^2 - p_y^2]^{1/2}$, $z_1 = R_z + z/2$, $z_2 = R_z - z/2$ and $k_{\mathrm{F}}(z) = [3\pi^2\rho(z)]^{1/3}$ is the local Fermi momentum. Here $\Gamma[\rho(z)]$ denotes the local annihilation rate.

As it stands, equation (10) is impossible to calculate due to the factor $k_{\mathrm{F}}^{-3}(R_z)$, which causes divergence of the integral for $R_z \to \infty$. Nieminen *et al* (1984) and Brown *et al* (1987, 1988b) overcame this difficulty by imposing a cut-off in $\Gamma(\rho)$ by putting $\Gamma[\rho(z)] = 0$ for z greater than some z_c. However, it is difficult to substantiate this method on physical grounds (as has been explained in detail by Rubaszek (1989)). Moreover, the resulting annihilation characteristics are found to be strongly dependent on the cut-off position z_c (Brown *et al* 1987).

Recently Brown *et al* (1988a, b) published the results of atomistic calculations of a positron trapped at a monovacancy on an Al surface, performed within MDA. In these works the ACAR spectra calculated with and without cut-off of annihilation rate Γ are quoted. However, avoiding this cut-off would only be possible if at least the condition $|\psi_+(x_v, y_v, z_v + z)|^2/\rho(x_v, y_v, z_v + z) \to 0$ for $z \to \infty$ was fulfilled, where (x_v, y_v, z_v) is the position of the vacancy. This means that the positron is so strongly localised *perpendicular* to the surface at the vacancy that it is not extended to the vacuum. If the vacancy is located in the second or in one of the next atomic layers, the requirement of convergence of MDA integrand is obviously fulfilled because in this case the formalism used in the papers by Brown *et al* (1988a, b) reduces the problem to trapping of a positron in a vacancy in the bulk material (cf., e.g. Arponen *et al* 1973). These results, however, could not be compared with the slow-positron experimental data. If the vacancy is located in the first atomic layer, the situation is different. Nieminen and Puska (1983) performed atomistic calculations of the electron and positron distributions in the neighbourhood of a monovacancy located in the first atomic layer of an Al(110) surface (this formalism is used in the papers by Brown *et al* (1988a, b) as well). According to the

results of Nieminen and Puska (1983) the positron wavefunction $\psi_+(x_v, y_v, z)$ is more extended to the vacuum (perpendicular to the surface) than the electron density $\rho(x_v, y_v, z)$ (see figure 2 of the paper by Nieminen and Puska). Avoiding the cut-off of local annihilation rate Γ, while calculating ACAR spectra within MDA, would only be possible if in the neighbourhood of the vacancy the positron wavefunction vanished in the vacuum more rapidly than the electron density, in contradiction to the results of Nieminen and Puska (1983). Unfortunately, Brown *et al* (1988a, b) do not present electron and positron distributions and therefore it is difficult to judge how far the requirement of convergence of MDA integrand is satisfied. The uncertainty about the calculations of Brown *et al* (1988a, b) is also connected with the fact that the conclusions of the 1988a paper are in disagreement with those of the 1988b paper, while some conclusions of both 1988 papers contradict the previously published ones (Brown *et al* 1987). Finally it should be stressed that, in spite of the defected surface, for the ideal metal surface the MDA integrand diverges if the cut-off in the local annihilation rate Γ is not imposed.

Another problem, connected with the applicability of the MDA to the surface problem, should be discussed. The simplest test for any approach enabling us to calculate ACAR spectra is IPM, imposing no enhancement of electron density on the positron. Within MDA, IPM calculations reduce to using, in equation (10), the free Sommerfeld annihilation rate in the form

$$\Gamma[\rho(z)] = \pi r_0^2 c\rho(z) \simeq 16\pi k_F^3(z)/3.$$

Of course, if the annihilation rate is applied in this form, no divergence in expression (10) occurs, in contrast to the enhanced model (where $\Gamma[\rho(z)] \to 2$ if $\rho(z) \to 0$). We computed one-dimensional IPM distributions $N(p_\parallel)$ according to formulae (9) and (10) and found significant differences, as discussed in § 3.2. Therefore, for the surface problem, MDA is not consistent with the definition of momentum distribution of annihilating pairs, given by formulae (8) or (9), because it uses improper electron wavefunctions (this fact is explained on mathematical grounds by Rubaszek (1989)). For this reason a great deal of caution is necessary when comparing surface ACAR spectra obtained within MDA with those calculated within IPM according to the formula (9) as well as when drawing conclusions about the shape of ACAR spectra following from MDA.

The present approach allows one to avoid both problems, i.e. the convergence of the integrand expression and the consistency with the definition of ACAR distribution. The ACAR spectra are calculated in a different way, beyond MDA. We base our approach on the local-density approximation (LDA) introduced by Daniuk *et al* (1985, 1987). Within LDA the functions $\psi_k^{ep}(\boldsymbol{r}, \boldsymbol{r})$ in ACAR formula (8) are obtained from the definition of momentum-dependent enhancement factors $\varepsilon(\boldsymbol{k}, \boldsymbol{x}_p)$ introduced by Kahana (1963):

$$\varepsilon(\boldsymbol{k}, \boldsymbol{x}_p) = \frac{|\psi_k^{ep}(\boldsymbol{x}_p, \boldsymbol{x}_p)|^2}{|\psi_k^0(\boldsymbol{x}_p)|^2 |\psi_+(\boldsymbol{x}_p)|^2}. \tag{11}$$

Thus, the particular electronic states are enhanced separately and locally, including an enhancement factor to the integrand. From formulae (1), (7), (8) and (11) we obtain

$$N(\boldsymbol{p}) = \int_0^\gamma \mathrm{d}k_z \left| \int_{-\infty}^{\infty} \exp(-\mathrm{i}p_z z)\psi_+(z)\psi_{k_z}(z)[\varepsilon((p_x^2 + p_y^2 + k_z^2)^{1/2}, r_s(z))]^{1/2}\, \mathrm{d}z \right|^2. \tag{12}$$

It should be stressed here that the enhancement factors ε in formula (12) need not

be the ones following from the Kahana theory. Others, more appropriate for the surface problem, should be used in (12) if available (see also remarks of Rubaszek (1989)).

It can be seen that the electron–positron enhancement factors ε are dependent not only on the local electron density (as in MDA) but also on the electronic state k_z. Therefore, the electron–positron pair wavefunctions are enhanced separately for particular electronic states, while within MDA only locally so. The main difference, however, is in using exact electron wavefunctions $\psi_k(z)$ instead of plane waves assumed in MDA (the detailed discussion is given in Rubaszek (1989)).

When formula (12) is used instead of (10) no divergence of the integrand occurs as $z \to \infty$. This follows from the fact that, although $\varepsilon(\boldsymbol{p}, r_s(z))$ is of order $[r_s(z)]^3$ and therefore tends to infinity if $r_s \to \infty$, nevertheless $[\psi_{k_z}(z)]^2$ is of order $[r_s(z)]^{-3}$ (cf. equation (5); $[r_s(z)]^3$ is the inverse of the local electron density $\rho(z)$). Thus, for $z \to \infty$ the product of $[\varepsilon(\boldsymbol{p}, r_s(z))]^{1/2}$ and $\psi_{k_z}(z)$ converges to a constant, dependent on p and k_z. This feature was also checked numerically up to $r_s(z) = 300$. The function $\psi_+(z)$ is normalised (to unity) and $|\exp(ip_z z)| = 1$, so the whole expression is without doubt integrable over the z axis. Moreover, this formalism is consistent with classical IPM formula (9): putting $\varepsilon = 1$ in formula (12) we simply switch to formula (9). The other advantages of the present formalism will be discussed in § 3.2.

The total annihilation rate λ, being the inverse of positron lifetime τ (i.e. $\lambda = 1/\tau$), was calculated in two equivalent ways, from the formula

$$\lambda_1 = (r_0^2 c/8\pi^2) \int N(P)\, \mathrm{d}\boldsymbol{p} \tag{13a}$$

or directly from

$$\lambda_2 = \int [\psi_+(z)]^2 \Gamma(z)\, \mathrm{d}z \tag{13b}$$

where

$$\Gamma(z) = (2r_0^2 c/\pi) \int_0^{k_F} \mathrm{d}k_z\, [\psi_{k_z}(z)]^2 \int_{k_z}^{k_F} t\varepsilon(t, z)\, \mathrm{d}t. \tag{13c}$$

Equations (13*b*) and (13*c*) are similar to those coming from the MDA and lead to similar results. However, this is not so with ACAR spectra. The detailed discussion will be given in § 3.2.

In our calculations (equations (12) and (13)) the momentum-dependent enhancement factors $\varepsilon(p)$ obtained within fully self-consistent Kahana theory (Rubaszek and Stachowiak 1988) were used.

3. Results and discussion

3.1. Electronic properties of Al surface

The electron density profile at the Al surface, $\rho(z)$, as well as the potentials V_{eff} and V_C, obtained self-consistently from equations (2)–(5) in the way presented in § 2.1, are

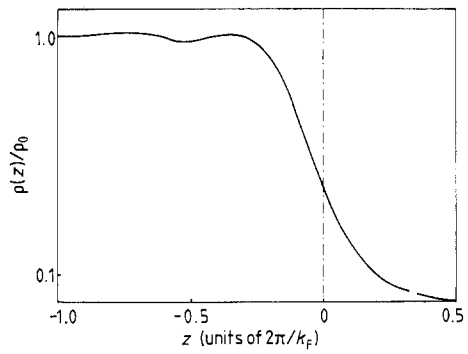

Figure 1. Electron density profile at an Al surface, $\rho(z)/\rho_0$, obtained self-consistently from equations (2)–(5).

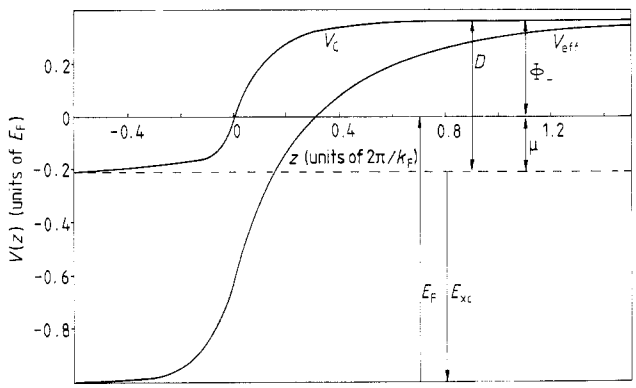

Figure 2. The effective electron potential V_{eff} and its Coulomb part V_C.

Table 1. The values of electron work function Φ_- and electrostatic dipole barrier D obtained within various electron–gas theories (all values in electronvolts).

	This work	Smith (1969)	Lang and Kohn (1971)	Monnier and Perdew (1978)	Experiment (Fomenko 1966)
D	6.59	6.03	6.26	6.24	–
Φ_-	4.223	3.64	3.87	3.88	4.25

shown in figures 1 and 2, respectively. Friedel oscillations of ρ near the surface are observed. It should be noted here that these oscillations, having a crucial effect on the values of the electron work function Φ_- and dipole barrier D, were completely neglected in Smith's (1969) calculations. Lang and Kohn's (1971) formalism leads to oscillating electron profiles; nevertheless the values of the work function resulting from their computations are found to be appreciably lower than experimental ones (cf. table 1).

The electron work function Φ_- is one of the most important surface parameters, characteristic of a given metal. It is usually defined as the minimum energy necessary to eject an electron from the metal and is given by

$$\Phi_- = D - \mu.$$

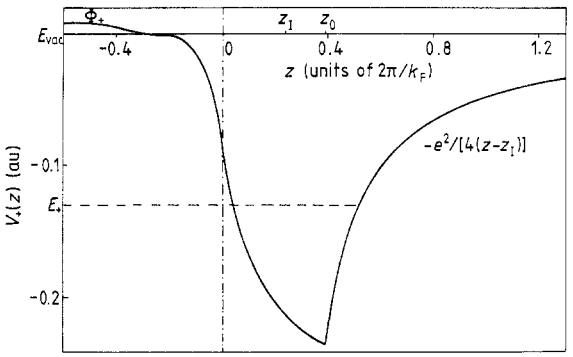

Figure 3. The positron potential V_+. The image plane is located at $z_1 = 1.6$ au. The image potential intersects the correlation part at $z_0 = 2.665$ au.

Here μ is the bulk chemical potential and D is the electronic relaxation surface dipole barrier calculated according to the formula

$$D = V_C(\infty) - V_C(-\infty) = 4\pi \int_{-\infty}^{\infty} z[\rho(z) - \rho_{ion}(z)]\,dz.$$

All these quantities are illustrated in figure 2. The values of Φ_- and D obtained for Al within various electron-gas theories are compared with experimental data in table 1. The present results are found to be in reasonable agreement with experiment.

Here a remark should be made. As is well known, real metals differ from an electron gas and the surface parameters are strongly dependent on the crystal face. Fortunately, the results for the Al(100) face are quite close to those obtained within the jellium model (Monnier and Perdew 1978). As concerns the other faces, band-structure calculations are required. The fact that for the Al(100) surface the jellium model seems to be a reasonable approximation encouraged us to consider our calculations as reliable ones, the more so as the experiment of Lynn *et al* (1985) was performed for the Al(100) face.

3.2. Annihilation characteristics

The positron potential V_+ and the positron wavefunction ψ_+ obtained in this work are presented in figures 3 and 4, respectively. The value of the binding energy (relative to vacuum), $E_B = -3.12$ eV, is in reasonable agreement with the experimental one, -3.03 ∓ 0.05 eV (Mills 1983 and references quoted therein). It should be pointed out that the calculations of ψ_+ were also performed for non-shifted image potential ($z_1 = 0$). However, in this case the result for $E_B = -1.86$ eV seemed to be very poor and we abandoned this model.

The resulting two-dimensional momentum distribution

$$N(p_\parallel, p_\perp) = \int N(\boldsymbol{p})\,dp_x$$

as well as the one-dimensional projections

$$N(p_\parallel) = \int N(p_\parallel, p_\perp)\,dp_\perp$$

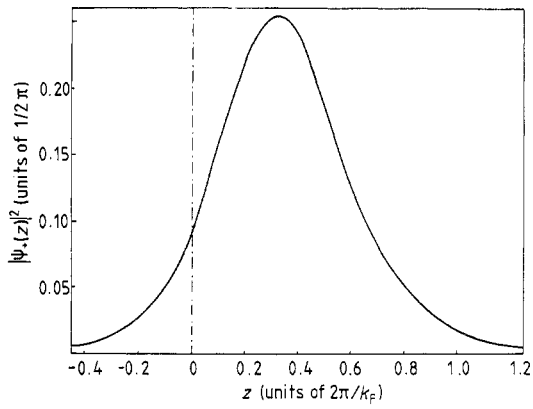

Figure 4. The positron density $|\psi_-(z)|^2$.

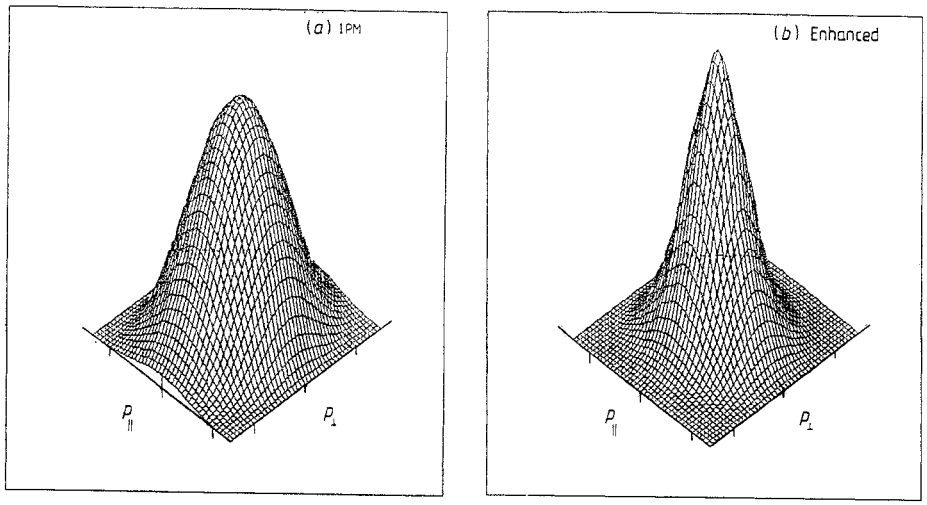

Figure 5. Two-dimensional momentum distributions $N(p_\parallel, p_\perp)$ obtained within IPM and enhanced model according to equations (9) and (12), respectively. The right-hand direction corresponds to $p_\perp$ and the left-hand one to $p_\parallel$. Momenta are expressed in units of milliradians.

and

$$N(p_\perp) = \int N(p_\parallel, p_\perp)\, \mathrm{d}p_\parallel$$

calculated within the IPM (equation (9)) and the fully correlated model (equation (12)) are presented in figures 5 and 6, respectively. In figure 6 the spectra are normalised to the same peak height. In figure 6 $N(P_\perp)$ are denoted in both cases (IPM and enhanced) by full curves and $N(p_\parallel)$ by broken curves. The bulk material (isotropic) spectra are quoted for comparison and are given by dotted curves. We also quote (shown by the chain curve) the values of $N(p_\parallel)$ obtained within MDA for IPM in the way described in § 2.3. Remarkable differences between the values of $N(p_\parallel)$ obtained according to formulae (9) and (10) are seen. This shows that MDA is not consistent with the definition of ACAR distribution in the case of metal surfaces, and a great deal of caution is necessary in drawing any conclusions about surface spectra from this formalism.

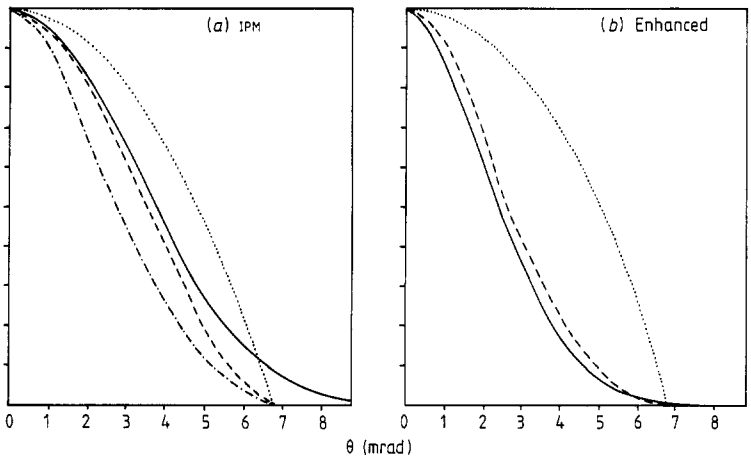

Figure 6. One-dimensional momentum distributions $N(p_\perp)$ (full curve) and $N(p_\parallel)$ (broken curve) obtained within IPM and enhanced models. The inverted parabola, corresponding to bulk material, is denoted by the dotted curve. The chain curve corresponds to $N(p_\parallel)$ obtained within MDA (formula (10)) for IPM.

In figures 5 and 6 it can be seen that including electron–positron correlations causes narrowing of ACAR spectra and *reverses* anisotropy. Let us introduce, for convenience, the anisotropy factor η, defined as the ratio of FWHM of $N(p_\perp)$ to FWHM of $N(p_\parallel)$. The isotropic ACAR spectra are characterised by $\eta = 1$. In our calculations the factor η decreases from IPM value $\eta^{\mathrm{IPM}} = 1.10$ to $\eta^{\mathrm{enh}} = 0.91$ in the enhanced model. This change of the anisotropy direction, although predicted by Lynn *et al* (1985) (cf. ref. 15 of their work while the position of $p_z = 0$ is moved), is the first theoretical one in the literature.

Anisotropy of ACAR spectra in both models, i.e. enhanced and IPM, still occurs (within 9% and 10%, respectively). Here a more detailed discussion is necessary. The FWHM of $N(p_\parallel)$ and $N(p_\perp)$ are narrower in the enhanced model than in IPM. The relatively stronger narrowing of $N(p_\perp)$ in the enhanced model is the main reason for the change of anisotropy direction. In our opinion the enhancement of electron density on the positron site (and therefore narrowing of $N(p_\perp)$) is overestimated. It should be remembered that, in our computations, Kahana-type momentum-dependent enhancement factors were used. On the other hand, one of the basic assumptions of Kahana's (1963) approach is that there is a spherically symmetric shape of the electronic screening charge around a positron (Kahana 1963, Rubaszek and Stachowiak 1988). This assumption is not valid near the metal surface. The strong electric field due to the surface dipole barrier distorts the screening cloud distribution around a positron located near the surface or outside the metal. Screening electrons are pulled off from the positron and attracted to the metal. Of course, the total screening charge is conserved but the density of electrons on the positron site decreases. Therefore, the momentum-dependent local enhancement factors $\varepsilon(p, z)$ and local annihilation rates $\Gamma(z)$ are diminished. Thus, there is a real need to determine the theoretical values of $\varepsilon(p, z)$ and $\Gamma(z)$. Preliminary calculations of screening charge distribution around a positron moving from the metal to vacuum were performed by Inglesfield and Stott (1980) within the random-phase approximation (RPA) and by Jensen and Walker (1988) based on weighted-density approximation (WDA).

These authors proved the decrease of electron density on the positron as the positron approaches the metal surface. According to the remarks of Inglesfield and Stott (1980), 'the polarisation cloud, which is spherical in the bulk, distorts and is left behind as the positron approaches the surface; as the positron leaves the metal the cloud flattens along the surface and becomes the classical image charge . . . as the positron approaches the surface the polarisation cloud becomes detached'. It was concluded that the positron almost completely 'loses' its screening cloud on leaving the metal. In our opinion the results are not so dramatic but generally they are apparently correct. It is well known that the RPA, used by Inglesfield and Stott (1980), does not give a satisfactory account of electron–positron correlations even in the range of metallic densities (it is correct for high densities only). In contrast to the results of Inglesfield and Stott, the screening cloud calculated by Jensen and Walker (1988) is never completely detached from a positron. According to the formalism of Jensen and Walker, the density of electronic screening charge on the positron (located at $\boldsymbol{r}$) is equal to $\rho(\boldsymbol{r})[\frac{5}{3} + (8\pi n(\boldsymbol{r}))^{-1}]$, where n is an effective electronic density obtained within WDA. This fact, however, could be attributed to the lack of self-consistency in the approach. Therefore, self-consistent calculations of screening charge around the surface positron are necessary. These calculations are just in the course of being performed.

From these remarks it follows that the Kahana-type enhancement factors, and any others obtained for the bulk material, are overestimated for the surface problem. Moreover, it was verified by us that decreasing values of $\varepsilon(p, z)$ cause a decrease of anisotropy. In this test the real values of $\varepsilon(p, r_s(z))$ were replaced by their biparabolic approximation

$$\varepsilon(p, r_s) \simeq a(r_s) + b(r_s)p^2 + c(r_s)p^4.$$

This slight underestimation of ε (Rubaszek and Stachowiak 1985) increases the anisotropy factor η by about 1%. It should be remembered that within the enhanced model the anisotropy is reversed with respect to IPM. This means that we switch from $\eta^{\mathrm{IPM}} > 1$ (resulting from any other theories) to $\eta^{\mathrm{enh}} < 1$ when the local enhancement factor (equation (12)) is applied. This, as well as the increase of η when ε is diminished, allows us to conclude that the present approach leads to isotropic ACAR spectra (characterised by the value $\eta = 1$) only if proper local momentum-dependent enhancement factors are used.

The ACAR spectra obtained within the present formalism are narrower than experimental ones (FWHM of $N(p_\perp)$ and $N(p_\parallel)$ are equal to 4.86 and 5.27 mrad, respectively, versus the experimental value of 7.1 mrad) but in close agreement with the theoretical result of Platzman and Tzoar (1986) (FWHM = 4.8 mrad). This discrepancy between the theoretical and experimental results could be attributed to a few reasons. First, there is the electron-gas model used in this work. However, this objection should not be treated literally because the electronic properties of the Al(100) face are very close to those of a jellium surface (Monnier and Perdew 1978). More problematic is the way in which the positron potential and the positron wavefunction are determined. These calculations are not self-consistent and the results for $\psi_+(z)$ are as reasonable as the approximations used for computing it. The position of the image plane, z_I, and the form of the electron–positron correlation energy E_{corr} could affect the positron wavefunction as well. The enhanced ACAR spectra are strongly dependent on the values of $\psi_+(z)$ (cf. equation (12)) and they are too narrow. On the other hand, the agreement between the resulting binding energy E_B and the experimental value substantiates the model used in the present work. Without doubt the self-consistent calculation of $\psi_+(z)$ is desired and

the two-component density-functional theory (cf., e.g. Lundqvist and March 1983, Chakraborty 1982, Boroński and Nieminen 1985) seems to be promising in this case (cf. also Jensen and Walker 1988).

The steps, vacancies and irregularities of the surface are neglected in our formalism whereas in real metals they should occur. Therefore, this difference between experimental and theoretical FWHM should not be discouraging.

The positron lifetime at an Al surface was computed by us in two numerically different ways: according to formulae (13*a*) and to (13*b*)–(13*c*). The resulting values were equal to $\tau_1 = 420$ ps and $\tau_2 = 405$ ps, respectively. The roughly 4% difference between τ_1 and τ_2 is due to minor numerical errors.

Both τ_1 and τ_2 are significantly shorter than the experimental value $\tau_{exp} = 580$ ps (Lynn *et al* 1984). Here the arguments concerning the values of $\varepsilon(p, r_s)$ should be quoted once again. Outside the surface the screening cloud is polarised, losing its spherically symmetric shape. Therefore, the positronium-like system is more like an excited P state than the ground S state. In the classical spherically symmetric system the density of electrons on the positron site cannot be less than that corresponding to the free positronium, and therefore the (local) lifetime is limited by $\tau_0 = 500$ ps. Near the surface the positronium S state is mixed with the excited P state (Platzman and Tzoar 1986), and for this reason the lifetime increases. Diminishing the values of local enhancement factors ε (which are overestimated) increases the positron lifetime. Here, also, reliable calculations of the electronic cloud screening the surface positrons are necessary. Finally it should be added here that the recent calculations of total annihilation rate performed by Jensen and Walker (1988) cannot be treated as definitive ones and, in our opinion, should be treated as quantitative only because of the lack of self-consistency in the formalism.

4. Conclusions

In the present work the ACAR spectra for positrons trapped at an ideal Al surface are determined within the correlated electron–positron model based on self-consistent calculations of electron density profiles within the jellium model. The electronic properties of the Al surface resulting from the presented approach are found to be in reasonable agreement with experimental data. According to the remarks of Monnier and Perdew (1978) the jellium model seems to be satisfactory for investigating the Al(100) face. Nevertheless, including the potential of the lattice would obviously improve our formalism. Particularly, abandoning the one-dimensional model and switching to the three-dimensional one would enable us to investigate, for example, defects of the surface (Brown *et al* 1988a, b). This problem, however, is very complicated numerically and we suppose it is still open. On the other hand, our calculations are only approximate and, in order to make real progress, first of all the self-consistent positron model should be introduced. Namely, the method of determining $\psi_+(z)$ and $V_+(z)$ should be modified (cf. Jensen and Walker 1988). Also the Kahana-type local momentum-dependent enhancement factors $\varepsilon(\boldsymbol{p}, r_s)$ should be replaced in formula (12) by their surface analogues. Calculations of the surface enhancement factors are now in progress.

Despite its deficiencies, the present formalism seems to be advantageous because it leads to quantitatively correct results for ACAR spectra. First of all, applying the local enhancement factors causes a relatively strong narrowing of $N(p_\perp)$ up to reversing the anisotropy, giving $N(p_\parallel)$ broader than $N(p_\perp)$ (while in IPM it is narrower—cf. figure 6).

The resulting ACAR spectra are only slightly anisotropic and diminishing the values of momentum-dependent enhancement factors (which are overestimated) allows one to cancel anisotropy and to obtain isotropic ACAR from the Al surface, in agreement with the experiment of Lynn *et al* (1985). The reversal of anisotropy obtained in this work (for the first time theoretically in the literature), leading to an isotropic shape of ACAR spectra, seems to be an unexpected feature because in the jellium model the positron is only localised perpendicular to the surface and it is completely extended in the surface plane. Since including local electron–positron correlations in the formalism (equation (12)) decreases the anisotropy factor η in comparison with its IPM value $\eta^{IPM} \geqslant 1$, we suppose that the isotropic shape of the experimental ACAR spectra should be attributed to these correlations. On the other hand, there is the question of which of the two features of $\varepsilon(\boldsymbol{k}, \boldsymbol{r})$ in formula (12)—their selectivity (momentum dependence) or locality (r dependence)—is the more responsible for this decrease of anisotropy factor. This will be investigated in our future work. Finally it should be stressed here that our conclusions disagree with those drawn by Brown *et al* (1987, 1988a, b). This is due to the fact that these authors compared the spectra obtained within two different formalisms: IPM spectra were calculated by Brown *et al* according to the exact ACAR formula (9) with proper electron wavefunctions while in the enhanced model (equation (10)) plane waves were used, instead of $\psi_{\boldsymbol{k}}(\boldsymbol{r})$, in formula (8) (cf. also Rubaszek 1989). If surface ACAR spectra calculated according to MDA formula (10) with Brand–Reinhaimer annihilation rate (enhanced model) were compared with those obtained from (10) with Sommerfeld annihilation rate (IPM), a decrease of anisotropy would occur as well.

Another point is how far the IPM result is model-sensitive, since the 10% anisotropy of IPM ACAR spectra can be compared with 9% reversed anisotropy of the enhanced model. In the region where the positron experiences image forces, the electronic screening cloud should be completely detached from a positron and therefore no enhancement of electron density on the positron should occur ($\varepsilon \equiv 1$), as within IPM. On the other hand, the positron wavefunction in ACAR formulae (equations (10) and (12)) is localised in the image–correlation well where electron–positron correlations are important and IPM is not satisfactory. If these correlations are neglected in the whole surface region, the resulting IPM positron lifetime, obtained according to formula (13*b*) with IPM annihilation rate $\Gamma^{IPM}(z) = 16\pi\rho(z)$ or according to (12) and 13*a*) with $\varepsilon \equiv 1$, must appreciably exceed the experimental value $\tau = 580$ ps (Lynn *et al* 1984). (Using our data for $\psi_+(z)$ and $\rho(z)$ in equation (13*b*) we have got the IPM positron lifetime equal to 5794 ps, i.e. one order of magnitude longer than the experimental one.) Therefore, although IPM could lead to less or more isotropic surface ACAR spectra, depending on the choice of electron and positron wavefunctions (Lou Yongming 1988, Brown *et al* 1988a, b), nevertheless the positron lifetime obtained within IPM is always overestimated and therefore IPM results cannot be treated as reliable. In contrast, the lifetime resulting from the enhanced model balances between its (overestimated) IPM value and its (underestimated) one corresponding to the use of bulk local partial (equations (12) and (13*a*)) or total (formula (13*b*)) annihilation rates. These conclusions are common for positron lifetime τ and anisotropy factor η (the latter is overestimated within IPM and underestimated if the local electron–positron correlations ε corresponding to the bulk material are used in equation (12)).

It is worthwhile to mention here that the experimental anisotropic ACAR from a Cu(121) surface, measured by Howell *et al* (1985), seems to confirm rather than contradict the present formalism. It should be remembered that copper is a transition metal and that the contribution of d electrons to the annihilation is significant. Recently it has

been found, both theoretically and experimentally (Singh *et al* 1986, Jarlborg and Singh 1987, Sormann 1987, 1988, Daniuk 1989a,b), that in transition metals the effect of de-enhancement occurs (this effect was first predicted by Fujiwara *et al* (1972)). The energy-dependent electron–positron local enhancement factors ε appeared to be decreasing functions of energy for some energy bands (especially d bands). For instance, in Ni, d states near the Fermi energy are not enhanced but effectively depressed (Singh *et al* 1986). De-enhancement effects are more pronounced where d electrons are present near the Fermi energy E_F (i.e. where E_F is near the top of the d band). It should be remembered that Cu is a typical metal in which the latter occurs. Therefore, in Cu, there is no reason for the strong relative narrowing of $N(p_\perp)$ to be as strong as in Al. Moreover, for Cu, the electron-gas model is obviously unsatisfactory and exact band-structure calculations are necessary. However, conceptual difficulties arise here. The conventional band-structure calculation methods (e.g. LAPW or LMTO) fall down because of violating the periodicity conditions near the metal surface. For determining $N(\boldsymbol{p})$ the effective energy-dependent local enhancement factors (Daniuk *et al* 1985, 1987) seem to be more appropriate.

As follows from these considerations, the problem of slow-positron interaction with clean metal surfaces is still open and this work is only an attempt to explain some experimental results. Al seems to be simple enough and therefore convenient for theoretical investigations but even in this case many unsolved questions remain. For more complicated metals, e.g. Cu, band-structure calculations are required. Surface defects, steps and irregularities create another field for theoretical investigations.

Acknowledgments

We are grateful to Dr Andy P Brown for numerical calculations of the positron wavefunction and to Dr Alison B Walker for critical remarks concerning anisotropy of IPM ACAR spectra. We would like to thank Dr Grażyna Kontrym-Sznajd and Dr Alfred Manuel for their valuable help in completing numerical calculations of ACAR spectra, as well as Professor Henryk Stachowiak for the scientific supervision of the work.

References

Arponen J, Hautojärvi P, Nieminen R and Pajanne E 1973 *J. Phys. F: Met. Phys.* **3** 2092–108
Bhattacharyya P and Singwi K S 1972 *Phys. Lett.* **41A** 457–60
Boroński E and Nieminen R M 1985 *Positron Annihilation* ed. P C Jain *et al* (Singapore: World Scientific) pp 100–3
Brown A P, Jensen Kjeld O and Walker A B 1988a *J. Phys. F: Met. Phys.* **18** L141–6
—— 1988b *Vacuum* **38** 409–11
Brown A P, Walker A B and West R N 1987 *J. Phys. F: Met. Phys.* **17** 2491–502
Canter K F, Mills A P Jr and Berko S 1974 *Phys. Rev. Lett.* **33** 7–10
Ceperley D M and Alder B J 1980 *Phys. Rev. Lett.* **45** 566–9
Chakraborty B 1982 *Positron Annihilation* ed. P G Coleman *et al* (Amsterdam: North-Holland) pp 207–9
Daniuk S 1989a *Acta Univ. Wratislav.* to appear
—— 1989b *J. Phys. Condens. Matter* **1** 5561–6
Daniuk S, Kontrym-Sznajd G, Mayers J, Rubaszek A, Stachowiak H, Walters P A and West R N 1985 *Positron Annihilation* ed. P C Jain *et al* (Singapore: World Scientific) pp 43–4 and 279–81
Daniuk S, Kontrym-Sznajd G, Rubaszek A, Stachowiak H, Mayers J, Walters P A and West R N 1987 *J. Phys. F: Met. Phys.* **17** 1365–78
Dupasquier A and Zecca A 1985 *Riv. Nuovo Cim.* **8** (ser 3) 1–73

Ewertowski R and Świątkowski W 1987 *Phys. Status Solidi* b **102** 555–7; *Phys. Scr.* **35** 745–6
Fomenko V S 1966 *Handbook of Thermionic Properties* (New York: Plenum)
Fujiwara K, Hyodo K T and Ohyama J 1972 *J. Phys. Soc. Japan* **33** 1047–59
Gunnarson O, Johnson O and Lundqvist B I 1979 *Phys. Rev.* B **20** 3136–64
Hodges C H and Stott M J 1973 *Solid State Commun.* **12** 1153–6
Howell R H, Meyer P, Rosenberg I J and Fluss M J 1985 *Phys. Rev. Lett.* **54** 1698–701
Inglesfield J and Stott M J 1980 *J. Phys. F: Met. Phys.* **10** 253–63
Jarlborg T and Singh A K 1987 *Phys. Rev.* B **36** 4660–3
Jensen K O and Walker A B 1988 *J. Phys. F: Met. Phys.* **18** L277–85
Kahana S 1963 *Phys. Rev.* **129** 1622–8
Lang N D and Kohn W 1971 *Phys. Rev.* B **3** 1215–33
Langreth D C 1972 *Phys. Rev.* B **5** 2842–3
Lou Yongming 1988 *Phys. Rev.* B **38** 9490–4
Lundqvist S and March N H (ed.) 1983 *Theory of the Inhomogeneous Electron Gas* (New York: Plenum)
Lynn K G, Frieze W E and Schultz P J 1984 *Phys. Rev. Lett.* **52** 1137–40
Lynn K G, Mills A P Jr, West R N, Berko S, Canter K F and Roelling L O 1985 *Phys. Rev. Lett.* **54** 1702–5
Manninen M, Nieminen R, Hautojärvi P and Arponen J 1975 *Phys. Rev.* B **12** 4012–22
Mills A P Jr 1983 *Positron Solid State Physics* ed. W Brandt and A Dupasquier (Amsterdam: North-Holland) pp 432–509
Mills A P Jr and Pfeiffer L N 1979 *Phys. Rev. Lett.* **43** 1961–4
Monnier R and Perdew J P 1978 *Phys. Rev.* B **17** 2595–611
Nieminen R and Manninen M 1974 *Solid State Commun.* **15** 403–6
Nieminen R and Puska M J 1983 *Phys. Rev. Lett.* **50** 281–4
Nieminen R, Puska M J and Manninen M 1984 *Phys. Rev. Lett.* **53** 1298–301
Pines D 1963 *Elementary Excitations in Solids* (New York: Benjamin) p 94
Platzman P M and Tzoar N 1986 *Phys. Rev.* B **33** 5900–3
Rozenfeld B, Jerie K and Świątkowski W 1983 *Acta Phys. Polon.* A **64** 93–105
Rubaszek A 1989 *J. Phys.: CM* **1** 2141–6
Rubaszek A and Stachowiak H 1985 *J. Phys. F: Met. Phys.* **15** L231–4
—— 1988 *Phys. Rev.* B **38** 3846–55
Singh A K, Manuel A A, Jarlborg T, Mathys Y, Walker E and Peter M 1986 *Helv. Phys. Acta* **59** 410–16
Smith J R 1969 *Phys. Rev.* **181** 522–9
Sormann H 1987 *Phys. Status Solidi* b **142** K45–8
—— 1988 *Acta Univ. Wratislav.* to appear; private communication
Walker A B and Nieminen R M 1986 *J. Phys. F: Met. Phys.* **16** L295–303
West R N 1974 *Positron Studies in Condensed Matter* (London: Taylor & Francis)